A Model-Based Approach for the Dynamic Calibration of Torque Transducers

Leonard Klaus, Michael Kobusch, Thomas Bruns

Physikalisch-Technische Bundesanstalt (PTB), Bundesallee 100, 38116 Braunschweig, Germany,
Tel: +49 531 592-1243, Fax: +49 531 592-69-1243, Email: leonard.klaus@ptb.de

This paper is the digital edition of a contribution at the *XXXIII IMAC – A Conference and Exposition on Structural Dynamics, Jan. 31 – Feb. 5, 2015*

The original reedited contribution can be found in *Proceedings of the 33rd IMAC, A Conference and Exposition on Structural Dynamics*, Volume 5: Sensors and Instrumentation, 2015, Springer, ISBN 978-3-319-15211-0.

A Model-Based Approach for the Dynamic Calibration of Torque Transducers

Leonard Klaus, Michael Kobusch, Thomas Bruns

Physikalisch-Technische Bundesanstalt (PTB), Bundesallee 100, 38116 Braunschweig, Germany
Email: leonard.klaus@ptb.de

ABSTRACT

The demand for traceable dynamic torque measurement has increased over the few last years. Procedures for the dynamic calibration of torque transducers have been developed in a European metrology research project. In the scope of this project, a dynamic measuring device was developed, and the corresponding mechanical modelling, which also includes the transducer under test, was investigated. The dynamic behaviour of the torque transducer is described by the parameters of its model. These model parameters will be identified from measurement data. The model-based approach for the description of the dynamic behaviour of torque transducers and model parameter identification procedures are described in this paper.

Keywords: Dynamic calibration, mechanical modelling, model parameter identification, dynamic measurement, dynamic torque calibration

NOMENCLATURE

Symbols

$\boldsymbol{D}$	damping matrix	$\mathrm{N \cdot m \cdot s/rad}$	λ	wavelength of light	m
f	frequency	Hz	φ	angle	rad
J	mass moment of inertia	$\mathrm{kg \cdot m^2}$	$\dot{\varphi}$	angular velocity	rad/s
$\boldsymbol{J}$	mass-moment-of-inertia matrix	$\mathrm{kg \cdot m^2}$	$\ddot{\varphi}$	angular acceleration	$\mathrm{rad/s^2}$
$\boldsymbol{K}$	torsional-stiffness matrix	$\mathrm{N \cdot m/rad}$	$\boldsymbol{\varphi}$	angle vector	rad
M	torque	$\mathrm{N \cdot m}$	$\dot{\boldsymbol{\varphi}}$	angular velocity vector	rad/s
$\boldsymbol{M}$	load matrix	$\mathrm{N \cdot m}$	$\ddot{\boldsymbol{\varphi}}$	angular acceleration vector	$\mathrm{rad/s^2}$
n	rotational speed	$\mathrm{s^{-1}}$	ω	angular frequency	$\mathrm{s^{-1}}$
P	mechanical power	W			
U	voltage	V			
t	time	s			

Abbreviations

DUT	Device under test
EMRP	European Metrology Research Programme
ICE	Internal combustion engine
LTI	Linear and time invariant
MMOI	Mass moment of inertia
ODE	Ordinary differential equation

1 INTRODUCTION

The demand for the traceable measurement of dynamic torque signals has increased over the last few years. Up to now, no traceable calibration procedures have existed. The same applies to other dynamic measurements of mechanical quantities, e.g. force and pressure. In the joint research project *Traceable Dynamic Measurement of Mechanical Quantities*, which was part of the European Metrology Research Programme (EMRP), nine national metrology institutes carried out joint research in the field of dynamic measurements from 2011 until 2014[1][2]. The investigation of the traceable dynamic calibration of torque transducers was part of this research project.

2 NEED FOR DYNAMIC CALIBRATION

Dynamic torque excitations exist in many fields of industry, but the greatest demand for dynamic calibration comes from the automotive industry. There are two important applications with dynamic torque signals which have suffered from the lack of traceability in particular: screw fastening tools and mechanical output power measurements.

Screw Fastening Tools

For the production of high quality industrial goods, automatic screw fastening systems are frequently used in assembly lines. They are supposed to fasten screw connections quickly to a specified torque. For safety-relevant connections, a traceable measurement of the fastening torque is necessary. Typical tools for this type of industrial application are impulse wrenches. They fasten the screw connection by applying a sequence of short impulses generated by the release of a pressurised hydraulic fluid. A typical torque pulse is depicted in Fig. 1. The steep pulses limit the operator's exposition to the high fastening torque due to the tools' inertia. Additionally, these tools feature short fastening times and good reproducibility of the fastening torque. The pulses are in the range of milliseconds and, therefore, have a frequency content of up to several hundred hertz in the torque output. The generated torque level can range from some newton metres to one kilonewton metre.

Mechanical Output Power Measurements

The mechanical output power P of internal combustion engines (ICE) as well as of electric motors can be measured by means of the rotational speed n and the torque M following

$$P = M \cdot n \quad . \tag{1}$$

The torque output of combustion engines is fluctuates highly over time. But electric motors generate dynamic torque components as well. Due to influences from power converters, high frequency torque components may appear in the torque output of electric motors (see Fig. 2). The frequency content of these dynamic components typically ranges from several hundred hertz, to some kilohertz both for ICEs and for electric motors. The torque output may amount up to several kilonewton metres.

The higher demands for low emission and for high efficiency, respectively, require a precise measurement of the output power of automotive ICEs, and of electric motors as well.

3 MEASURING DEVICE

The demands for higher precision in torque measurement require the comprehension of dynamic effects. In order to perform the dynamic calibration of torque transducers, a dedicated measuring device was developed[3]. The device and its working principle are depicted in Fig. 3.

The measurement principle is based on Newton's second law. The generated dynamic torque $M(t)$ can be measured by means of the angular acceleration $\ddot{\varphi}(t)$ and the mass moment of inertia (MMOI) J giving

$$M(t) = \ddot{\varphi}(t) \cdot J \quad . \tag{2}$$

The dynamic torque is generated by a rotational exciter using monofrequent sinusoidal signals. The mechanical design of the dynamic torque measuring device features a vertical drive shaft connected to further components in series arrangement,

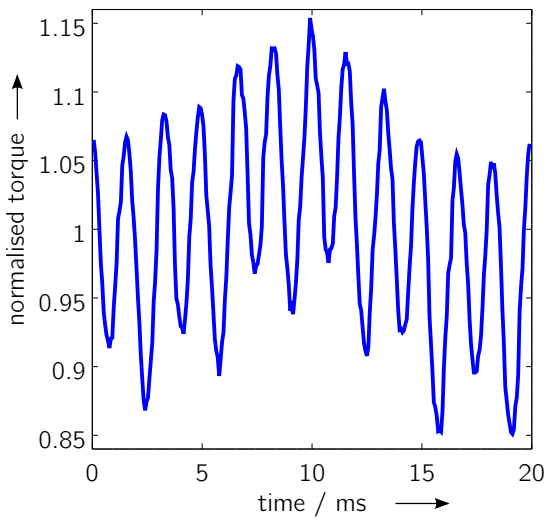

Figure 1: Torque output of an impulse wrench.

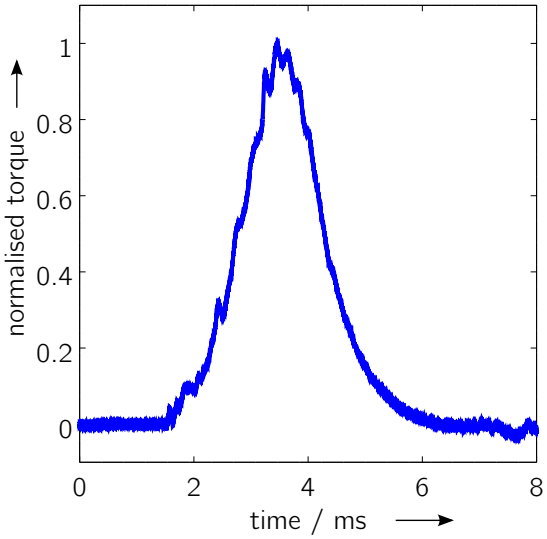

Figure 2: Torque output of an electric synchronous motor (courtesy of Working Group 3.52 of PTB).

which are exposed to the forced rotational excitation. At the bottom, the rotational exciter is mounted on an adjustable platform that can be moved vertically. The transducer under test (device under test, DUT) is mounted between two couplings above the rotational exciter. Both couplings are torsionally stiff but flexible to bending, in order to reduce influences from bending moments and lateral forces to the transducer under test. At the top end of the drive shaft, the arrangement of an air bearing and a radial grating disk enables a precise measurement of the time-dependent angular position providing low friction to the rotational oscillations. All components mounted at the top of the transducer under test contribute to the acting mass moment of inertia of Eq. 2.

The measurement of the angular position at the top is carried out by a rotational heterodyne Doppler interferometer measuring through the aforementioned radial grating disk. The two laser beams are diffracted by the grating lines, and the first diffraction order is coupled back into the interferometer. At each passing of a grating line, the laser beam with a wavelength λ exhibits a phase shift of 2π, which is analysed for the measurement.

The angular acceleration at the bottom of the transducer is measured by means of an angular accelerometer embedded in the rotor of the rotational exciter.

When carrying out measurements, the rotational excitations at the top and the bottom of the drive shaft are acquired simultaneously sampling the output voltage of the transducer successively for different excitation frequencies. These frequencies were chosen according to the recommendations of ISO 266[4]. All three acquired signals are approximated with a sine-fit of common frequency. For this purpose, the signals are normalised to avoid unwanted weighting effects due to the different numerical magnitudes of the acquired signals. The applied algorithm is a Levenberg-Marquardt nonlinear least squares approach.

4 MODEL

The dynamic behaviour of the torque transducer under test is described by an appropriate mechanical model. Such a model-based approach for dynamic calibration is necessary, because all torque transducers are coupled to their mechanical environment on both sides at the time of measurement. The mechanically coupled components may influence the transducer's dynamic behaviour.

The model of the transducer is linear and time invariant (LTI). The assumption of LTI behaviour is valid, because the transducers are designed to be linear and stable over time. This has already been investigated for static calibration purposes. The majority of torque transducers use a measuring principle based on strain gauges, which leads to a characteristic

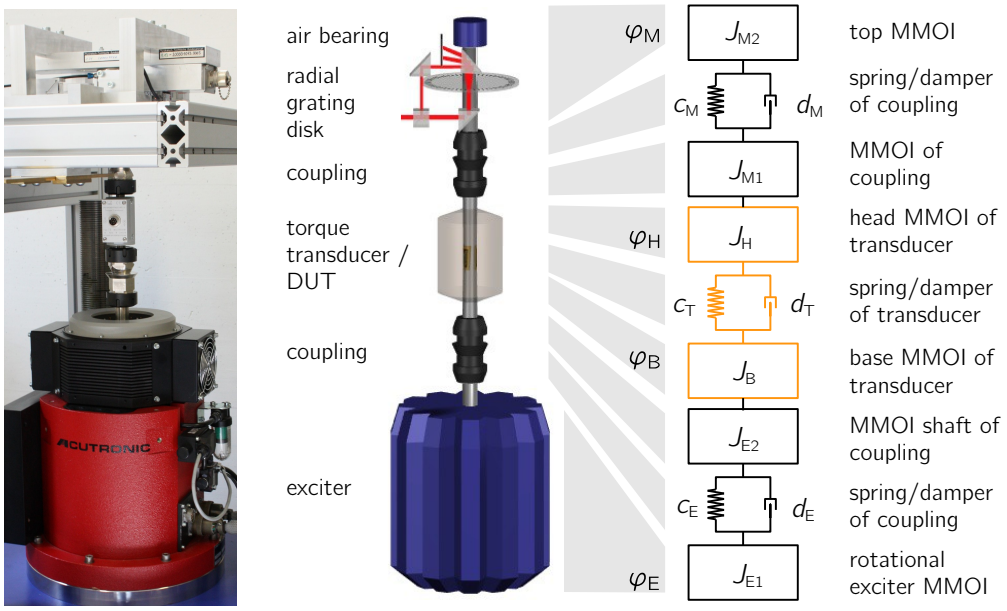

Figure 3: Dynamic torque measuring device (left), its schematic representation (middle) and model description (right), the components of the transducer are marked in orange, those of the measuring device are marked in black.

mechanical design. The transducers are designed to be torsionally stiff, but the measuring element sensing the strain generated by the acting torque is comparably compliant. Therefore, the basic model of the transducer consists of two rigid mass-moment-of-inertia elements connected by a torsional spring and a torsional damper in parallel (see Fig. 3).

To be able to identify the transducer's model parameters, the mechanical environment needs to be taken into account. Therefore, the basic model of the torque transducer was extended to a model of the transducer and the measuring device, which is – in case of the calibration – the mechanical environment. The extended model, which includes the measuring device and the transducer under test, is again LTI. The model components were chosen corresponding to the components of the measuring device, to establish a physical model of the whole measuring set-up.

5 MODEL PARAMETER IDENTIFICATION PROCEDURE

The calibration of the torque transducer under test is to be carried out by identifying its model parameters by means of measured data. To do so, a sufficiently low number of unknown parameters of the model is desired. Therefore, the model parameters of the measuring device need to be determined prior to the model parameter identification of the DUT as far as possible.

For the purpose of the identification of the model properties of the measuring device, three auxiliary measurement set-ups for the measurands torsional stiffness, mass moment of inertia[5] and rotational damping[6] were developed. With the measurement results from these set-ups, all required model parameters of the measuring device were determined. The known and unknown model parameters of the measuring device and of the device under test are given in Table 1.

Table 1: Model parameters of the measuring device and the transducer under test.

	known model parameters	unknown model parameters
mass moment of inertia	J_{M2}, J_{M1}, J_{E2}	J_{B}, J_{H}
torsional stiffness	c_{M}, c_{E}	c_{T}
damping	d_{M}, d_{E}	d_{T}

The model is mathematically described as an inhomogeneous ordinary differential equation system (ODE) giving

$$\boldsymbol{J} \cdot \ddot{\boldsymbol{\varphi}} + \boldsymbol{D} \cdot \dot{\boldsymbol{\varphi}} + \boldsymbol{K} \cdot \boldsymbol{\varphi} = \boldsymbol{M} \tag{3}$$

with the mass-moment-of-inertia matrix $\boldsymbol{J}$, the torsional-stiffness matrix $\boldsymbol{K}$ and the damping matrix $\boldsymbol{D}$. The angle vector $\boldsymbol{\varphi}$ describes the angle excitations at different positions in the model, the derivatives $\dot{\boldsymbol{\varphi}}$, $\ddot{\boldsymbol{\varphi}}$ the angular velocity and angular acceleration, respectively. The excitation by the rotational exciter is described by the load vector $\boldsymbol{M}$. For the model of the measuring device and the device under test, the resulting matrices are the following:

$$\boldsymbol{J} = \begin{bmatrix} J_{\mathrm{M2}} & 0 & 0 & 0 \\ 0 & (J_{\mathrm{M1}} + J_{\mathrm{H}}) & 0 & 0 \\ 0 & 0 & (J_{\mathrm{B}} + J_{\mathrm{E2}}) & 0 \\ 0 & 0 & 0 & J_{\mathrm{E1}} \end{bmatrix} \quad \boldsymbol{D} = \begin{bmatrix} d_{\mathrm{M}} & -d_{\mathrm{M}} & 0 & 0 \\ -d_{\mathrm{M}} & (d_{\mathrm{M}} + d_{\mathrm{T}}) & -d_{\mathrm{T}} & 0 \\ 0 & -d_{\mathrm{T}} & (d_{\mathrm{T}} + d_{\mathrm{E}}) & -d_{\mathrm{E}} \\ 0 & 0 & -d_{\mathrm{E}} & d_{\mathrm{E}} \end{bmatrix} \tag{4a}$$

$$\boldsymbol{C} = \begin{bmatrix} c_{\mathrm{M}} & -c_{\mathrm{M}} & 0 & 0 \\ -c_{\mathrm{M}} & (c_{\mathrm{M}} + c_{\mathrm{T}}) & -c_{\mathrm{T}} & 0 \\ 0 & -c_{\mathrm{T}} & (c_{\mathrm{T}} + c_{\mathrm{E}}) & -c_{\mathrm{E}} \\ 0 & 0 & -c_{\mathrm{E}} & c_{\mathrm{E}} \end{bmatrix} \tag{4b}$$

$$\boldsymbol{\varphi} = \begin{bmatrix} \varphi_{\mathrm{M}}(t) \\ \varphi_{\mathrm{H}}(t) \\ \varphi_{\mathrm{B}}(t) \\ \varphi_{\mathrm{E}}(t) \end{bmatrix} \qquad \dot{\boldsymbol{\varphi}} = \begin{bmatrix} \dot{\varphi}_{\mathrm{M}}(t) \\ \dot{\varphi}_{\mathrm{H}}(t) \\ \dot{\varphi}_{\mathrm{B}}(t) \\ \dot{\varphi}_{\mathrm{E}}(t) \end{bmatrix} \qquad \ddot{\boldsymbol{\varphi}} = \begin{bmatrix} \ddot{\varphi}_{\mathrm{M}}(t) \\ \ddot{\varphi}_{\mathrm{H}}(t) \\ \ddot{\varphi}_{\mathrm{B}}(t) \\ \ddot{\varphi}_{\mathrm{E}}(t) \end{bmatrix} \qquad \boldsymbol{M} = \begin{bmatrix} 0 \\ 0 \\ 0 \\ M(t) \end{bmatrix} \tag{4c}$$

Based on this ODE system, the unknown model parameters can be identified by means of the measurement data. For this purpose, it is recommended to acquire all angle positions, angular velocities and angular accelerations given in $\boldsymbol{\varphi}$, $\dot{\boldsymbol{\varphi}}$ and $\ddot{\boldsymbol{\varphi}}$. The excitation with harmonic oscillations (sinusoidal signals) with known angular frequencies $\omega = 2\pi f$ makes it possible to calculate the wanted angle quantities from one measured angle, angular velocity or angular acceleration and vice versa as follows

$$\begin{aligned} \varphi(t) &= \hat{\varphi}\, \mathrm{e}^{\mathrm{i}\omega t} \\ \dot{\varphi}(t) &= \mathrm{i}\omega\, \hat{\varphi}\, \mathrm{e}^{\mathrm{i}\omega t} = \mathrm{i}\omega\, \varphi(t) \\ \ddot{\varphi}(t) &= -\omega^2\, \hat{\varphi}\, \mathrm{e}^{\mathrm{i}\omega t} = -\omega^2 \varphi(t) \quad , \end{aligned} \tag{5}$$

where $\mathrm{i} = \sqrt{-1}$ denotes the imaginary number.

Technically it is not possible to acquire angle information at all desired positions given in $\boldsymbol{\varphi}$, $\dot{\boldsymbol{\varphi}}$ and $\ddot{\boldsymbol{\varphi}}$. The angle excitation at the top and the bottom of the transducer cannot be measured directly, but it can be derived from the output signal of the torque transducer. The output signal of the torque transducer is assumed – due to its linear behaviour – to be proportional to the input torque. Strain gauge transducers measure strain generated by torsion, therefore the output voltage is proportional to the angle difference $\Delta\varphi_{\mathrm{HB}}$ at the top and the bottom of the transducer.

$$U(t) \propto M(t) \propto \Delta\varphi_{\mathrm{HB}}(t) \quad . \tag{6}$$

Applying the proportionality parameter ρ gives the direct relation of the measured output voltage and the torsion of the transducer as

$$U(t) = \rho \cdot \Delta\varphi_{\mathrm{HB}}(t) \quad . \tag{7}$$

Two complex frequency response functions can be derived[7] from the acquired signals, which are shown in Fig. 4. The frequency response functions consist of the mechanical input of the top part or the bottom part of the measuring device and of the output of the transducer. For the response function of the top part of the measuring device $H_{\mathrm{top}}(\mathrm{i}\omega)$, the frequency response of the transducer output and angular acceleration at the top is calculated, and the frequency response of the bottom part of the measuring device $H_{\mathrm{bott}}(\mathrm{i}\omega)$ relates the output signal of the transducer and the angular acceleration of the bottom.

The corresponding model parameters for each of the input quantities of the frequency response functions can be derived from the ODE system (cf. Eqs. 3, 4a, 4b, 4c). These two frequency response functions comprise all unknown parameters of the device under test. It is possible to derive J_{H}, c_{T}, d_{T} and ρ from $H_{\mathrm{top}}(\mathrm{i}\omega)$ giving

$$H_{\mathrm{top}}(\mathrm{i}\omega) = -\rho \cdot \frac{J_{\mathrm{M2}} + (J_{\mathrm{M1}} + J_{\mathrm{H}}) \cdot K_{\mathrm{t}}(\mathrm{i}\omega)}{\mathrm{i}\omega d_{\mathrm{T}} + c_{\mathrm{T}}} \tag{8}$$

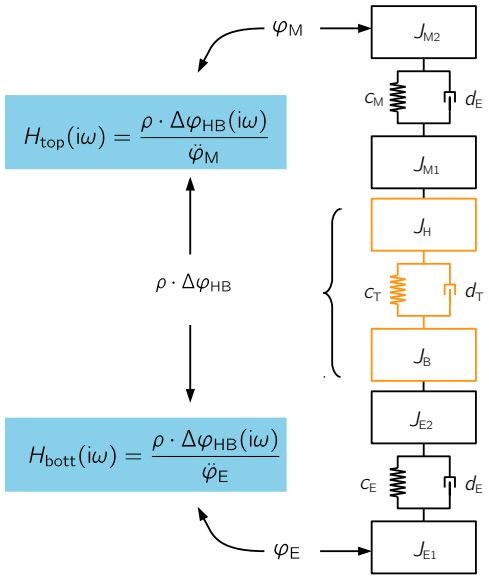

Figure 4: Transfer functions based on the acquired measurands.

whereby K_t is a set of known parameters of the top part of the measurement device

$$K_\mathrm{t}(\mathrm{i}\omega) = \frac{\varphi_\mathrm{H}}{\varphi_\mathrm{M}} = \frac{\omega^2\, J_\mathrm{M2} + \mathrm{i}\omega d_\mathrm{M} + c_\mathrm{M}}{\mathrm{i}\omega d_\mathrm{M} + c_\mathrm{M}} \quad . \tag{9}$$

With K_b consisting only of known parameters of the bottom part of the measuring device such as

$$K_\mathrm{b}(\mathrm{i}\omega) = \frac{\omega^2\, J_\mathrm{E2} + \mathrm{i}\omega d_\mathrm{E} + c_\mathrm{E}}{\mathrm{i}\omega d_\mathrm{E} + c_\mathrm{E}} \quad , \tag{10}$$

the transfer function of the bottom parts $H_\mathrm{bott}(\mathrm{i}\omega)$ gives

$$H_\mathrm{bott}^{-1}(\mathrm{i}\omega) = \frac{\omega^2}{\rho} \cdot \left(\frac{-\omega^2\, J_\mathrm{B}}{\mathrm{i}\omega d_\mathrm{E} + c_\mathrm{E}} + \frac{\mathrm{i}\omega d_\mathrm{T} + c_\mathrm{T}}{\mathrm{i}\omega d_\mathrm{E} + c_\mathrm{E}} + K_\mathrm{b}(\mathrm{i}\omega) \right) - \frac{K_\mathrm{t}(\mathrm{i}\omega)}{\rho} \cdot \left(\frac{\left(\frac{-\omega^2\, J_\mathrm{B}}{\mathrm{i}\omega d_\mathrm{E} + c_\mathrm{E}} + K_\mathrm{b}(\mathrm{i}\omega) \right) \cdot (\mathrm{i}\omega d_\mathrm{T} + c_\mathrm{T})}{J_\mathrm{M2} + (J_\mathrm{M1} + J_\mathrm{H}) \cdot K_\mathrm{t}(\mathrm{i}\omega)} \right) \quad . \tag{11}$$

For better readability, the inverse function $H_\mathrm{bott}(\mathrm{i}\omega)^{-1}$ is displayed. From this frequency response function, the unknown parameters J_H, J_B, c_T, d_T and ρ can be derived. Detailed information about the identification process is given in[7].

The model parameter identification can use least squares procedures and will be carried out in the frequency domain. Equations 8 and 11 for the system descriptions are the basis for the model parameter identification. The model is nonlinear in the parameters, which means that it will be necessary to use corresponding algorithms. Nonlinear regression problems cannot be solved directly, they require an iterative process for an estimation of the solution.

Both frequency response equations will be included in the parameter identification process and will be used together in one run. The parameter identification will be carried out with the complex measurement data both for the real and the imaginary parts of the frequency response equations.

6 INFLUENCES OF ELECTRONIC COMPONENTS IN THE MEASURING CHAIN

The data needed for the model parameter identification should contain only information of the mechanical system. Therefore, all influences from electronic components in the signal acquisition chain need to be measured first and then compensated for prior to the model parameter identification. This includes the measuring components for the measurement of angle and angular acceleration, signal conditioning amplifiers, filters and analogue-to-digital converters.

Angle Measurement / Angular Acceleration Sensor The measurement of the angle position is carried out by means of a heterodyne interferometer and software demodulation. With the software demodulation, influences from the electronics can be avoided, and the only remaining influences are the deviations in the grating, the laser wavelength λ and the precision of the time/frequency measurement.

The angular acceleration sensor was calibrated using primary methods. For this purpose, a prism was mounted at a known distance from the axis of rotation. The displacement of the prism was measured by interferometric methods.

Bridge Amplifiers The strain gauges in the transducers under test are arranged as a Wheatstone bridge. The signal conditioning of those circuits is carried out with bridge amplifiers. For the dynamic calibration of those amplifiers, a dynamic bridge standard was developed at PTB[8]. The dynamic bridge standard enables dynamic calibration in a frequency range from DC (0 Hz) up to 10 kHz.

The influences of the conditioning electronics need to be analysed not only for stand-alone bridge amplifiers used with passive torque transducers, but for transducers with integrated electronics as well. This may be difficult, because some transducers are sealed and access to the circuit board is not possible due to their mechanical design.

Analogue Digital Converters The analogue digital converters used for the voltage acquisition were calibrated with a Fluke 5700A calibrator. The timing of all channels was compared to PTB's distributed frequency standard.

For each component, the complex frequency response function $H(\mathrm{i}\omega)$ was calculated based on the calibration results with the input $X(\mathrm{i}\omega)$ and the output $Y(\mathrm{i}\omega)$ as

$$H(\mathrm{i}\omega) = \frac{Y(\mathrm{i}\omega)}{X(\mathrm{i}\omega)} \quad . \tag{12}$$

Based on the calibration results, the magnitude $A(\omega)$ and the phase $\varphi(\omega)$ of the complex frequency response can be derived giving

$$A(\omega) = |H(\mathrm{i}\omega)| = \sqrt{\mathrm{Re}\left(H(\mathrm{i}\omega)\right)^2 + \mathrm{Im}\left(H(\mathrm{i}\omega)\right)^2} \tag{13}$$

$$\varphi(\omega) = \arctan\left(\frac{\mathrm{Im}\left(H(\mathrm{i}\omega)\right)}{\mathrm{Re}\left(H(\mathrm{i}\omega)\right)}\right) \quad . \tag{14}$$

The measurement data Y_{meas} can now be corrected in the frequency domain either for magnitude A and phase φ

$$A_{\mathrm{corr}}(\omega) = A_{\mathrm{meas}}(\omega) \cdot A_{\mathrm{calib}}(\omega)^{-1} \quad \text{and} \quad \varphi_{\mathrm{corr}}(\omega) = \varphi_{\mathrm{meas}}(\omega) - \varphi_{\mathrm{calib}}(\omega) \quad , \tag{15}$$

or for complex signals

$$Y_{\mathrm{corr}}(\mathrm{i}\omega) = Y_{\mathrm{meas}}(\mathrm{i}\omega) \cdot H_{\mathrm{calib}}(\mathrm{i}\omega)^{-1} \tag{16}$$

applying a multiplication with the inverse complex frequency response function $H_{\mathrm{calib}}(\mathrm{i}\omega)$.

7 MEASUREMENT RESULTS

In preparation of the model parameter identification, measurements with different transducers were carried out. The chosen transducers have different mechanical designs, different torque capacities and, therefore, represent the whole range of transducers which could be calibrated in the dynamic torque measuring device.

Three different types of transducers were chosen (see Fig. 5).

Shaft type torque transducer of 1 N · m: This very low capacity transducer fits the measuring device's torque generation capabilities very well. However, it has non-contact signal conditioning and transmission electronics included, which cannot be calibrated without the complete disassembly of the transducer.

Shaft type torque transducer of 10 N · m: This passive transducer features direct access to the Wheatstone bridge via slip rings. It was possible to connect a dynamically calibrated bridge amplifier and, therefore, to correct for the amplifier's dynamic behaviour.

Flange type torque transducer of 50 N · m: This transducer has the highest capacity of the analysed transducers and has – due to its mechanical design – a high torsional stiffness and a large mass moment of inertia. The torque signals are conditioned by a bridge amplifier in the rotor and transmitted by a telemetry system. The electronic components of an identical transducer were calibrated, because the transducers are sealed and cannot be opened without causing damage. Based on the calibration data, the influences of the electronics can be corrected.

Figure 5: Analysed torque transducers, 1 N · m shaft type (left), 10 N · m shaft type (middle), and 50 N · m flange type (right).

The measurement results of the three analysed transducers are depicted in Figs. 6, 7 and 8. The frequency response functions for the top and for the bottom of each transducer are given in magnitude and in phase.

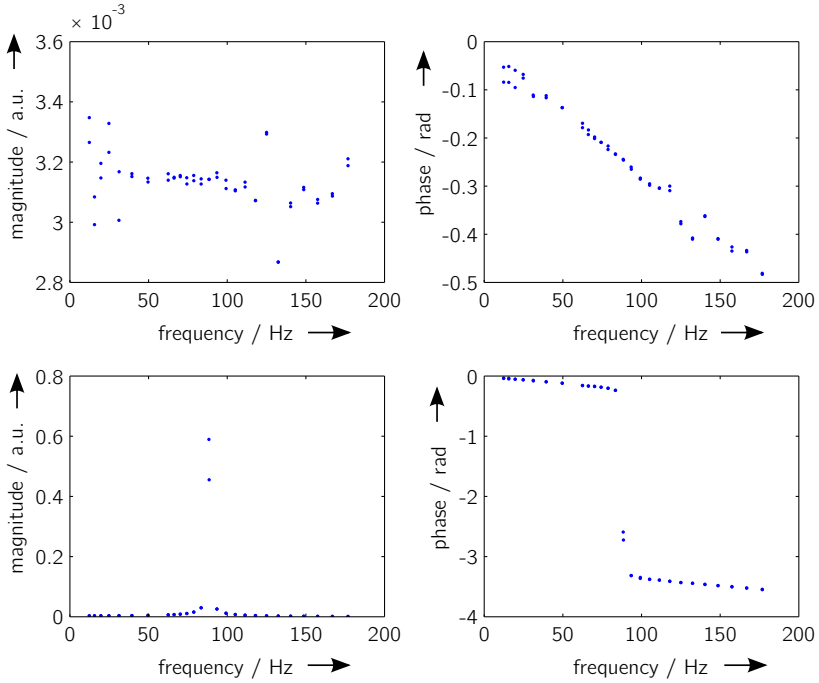

Figure 6: Frequency response function H_{top} (top) and H_{bott} (bottom) in magnitude and phase measured with a shaft type transducer of 1 N · m nominal load.

Each transducer was analysed in the dynamic torque measuring device. Depending on the properties (torsional stiffness, mass moment of inertia) of the transducer, the frequency response will behave in a characteristic manner. Frequencies higher than the resonance frequency of the drive shaft are difficult to excite because of a declining sensitivity at the top. The higher the frequency, the smaller is the relative magnitude at the top of the measuring device. Therefore, the practical frequency limit exists somewhat beyond the transducer's resonance frequency in the given configuration. Moreover, even before this limit is reached, the magnitudes of excitation at the top ($\ddot{\varphi}_{\mathrm{M}}$) will be very small and will show comparably high noise levels causing deviations in the sine fit results.

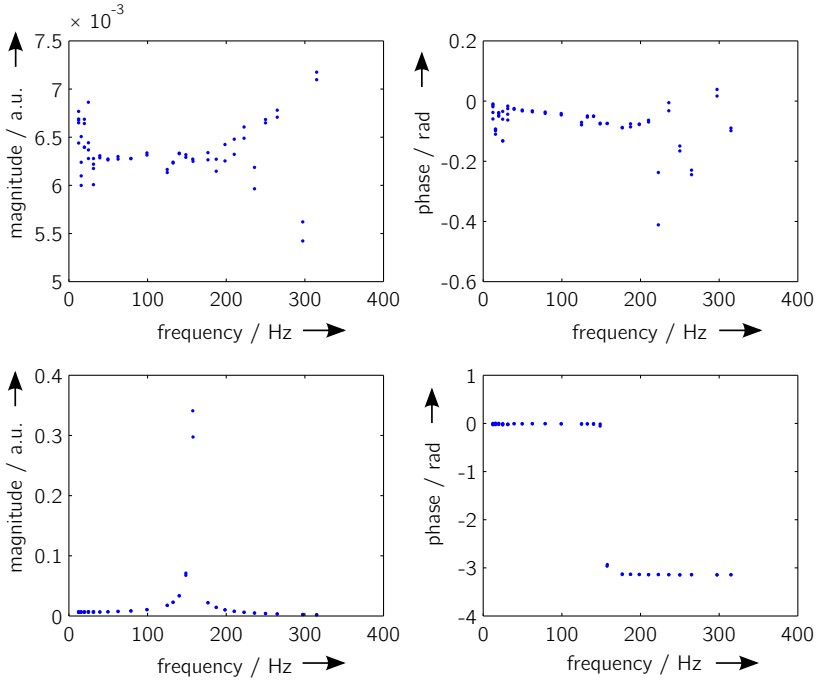

Figure 7: Frequency response function H_{top} (top) and H_{bott} (bottom) in magnitude and phase measured with a shaft type transducer of 10 N · m nominal load.

It becomes obvious from the experimental measurement results that knowledge about the influence of the signal conditioning electronics is essential. The frequency response function of the low capacity transducer (see Fig. 6) has, despite the comparably small range of excitation frequencies, clearly a phase lag which cannot be explained by mechanical influences. These effects cannot be found in the results of the two other transducers, where the influences from signal conditioning are compensated for.

8 SIMULATION RESULTS

The frequency response of the modelled system was analysed using calculated simulations. To this end, the two frequency response functions were calculated using Eqs. 8 and 11. The mechanical properties of the measuring device (i.e. the known model parameters from Table 1) were used to compute the frequency response functions with expected parameters of transducers. The result for the 10 N · m shaft type transducer can be found in Fig. 9.

A good agreement between the simulation results and the measurement was found. A sensitivity analysis of the resulting frequency response functions to changes in parameters showed that only those parameter changes which affect the frequency response function of the whole drive shaft correspondingly can be well identified[9]. The influence of the parameters of the device under test on the frequency responses are therefore dependent on the mechanical design of the measuring device as well.

9 CONCLUSIONS

The dynamic calibration of torque transducers is important for various applications in industry, in particular for efficiency measurement of electric motors and internal combustion engines, as well as for screw fastening tools with dynamic torque outputs.

In this paper, a model-based approach for the description of torque transducers, a measuring device and the corresponding

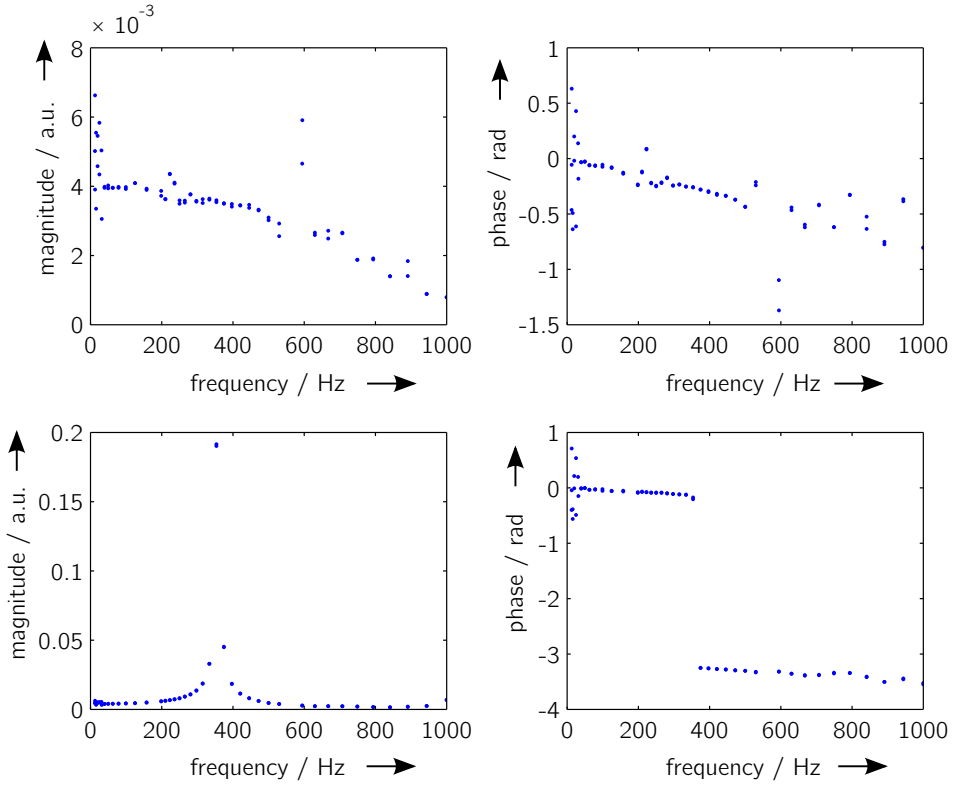

Figure 8: Frequency response function H_{top} (top) and H_{bott} (bottom) in magnitude and phase measured with a flange type transducer of 50 N · m nominal load.

model description of the transducer under test are presented. Procedures for the compensation of the effects of signal conditioning and transmission electronics are explained. The model parameter identification using two frequency response functions of the measuring device and a nonlinear least-squares approximation enables a determination of the properties of the transducer under test by means of measurement data. Dynamic measurement results of three torque transducers demonstrate the capability and limitations of the current measuring set-up. Calculations of simulated system responses confirm the model assumptions of a torsional spring-mass-damper system.

ACKNOWLEDGMENTS

The authors would like to thank their colleague Barbora Arendacká from Working Group 8.42 *Data Analysis and Measurement Uncertainty* of PTB for her helpful recommendations and the support in system simulation and model parameter identification.

This work is part of the Joint Research Project IND09 *Traceable Dynamic Measurement of Mechanical Quantities* of the European Metrology Research Programme (EMRP). The EMRP is jointly funded by the EMRP participating countries within EURAMET and the European Union.

REFERENCES

[1] **Bartoli, C. et al.**, *Traceable Dynamic Measurement of Mechanical Quantities: Objectives and First Results of this European Project*, International Journal of Metrology and Quality Engineering, Vol. 3, No. 3, pp. 127–135, May 2013.

[2] **Bartoli, C. et al.**, *Dynamic Calibration of Force, Torque and Pressure Sensors*, *Proc. of Joint IMEKO International TC3, TC5 and TC22 Conference 2014*, Cape Town, South Africa, Feb. 2014.

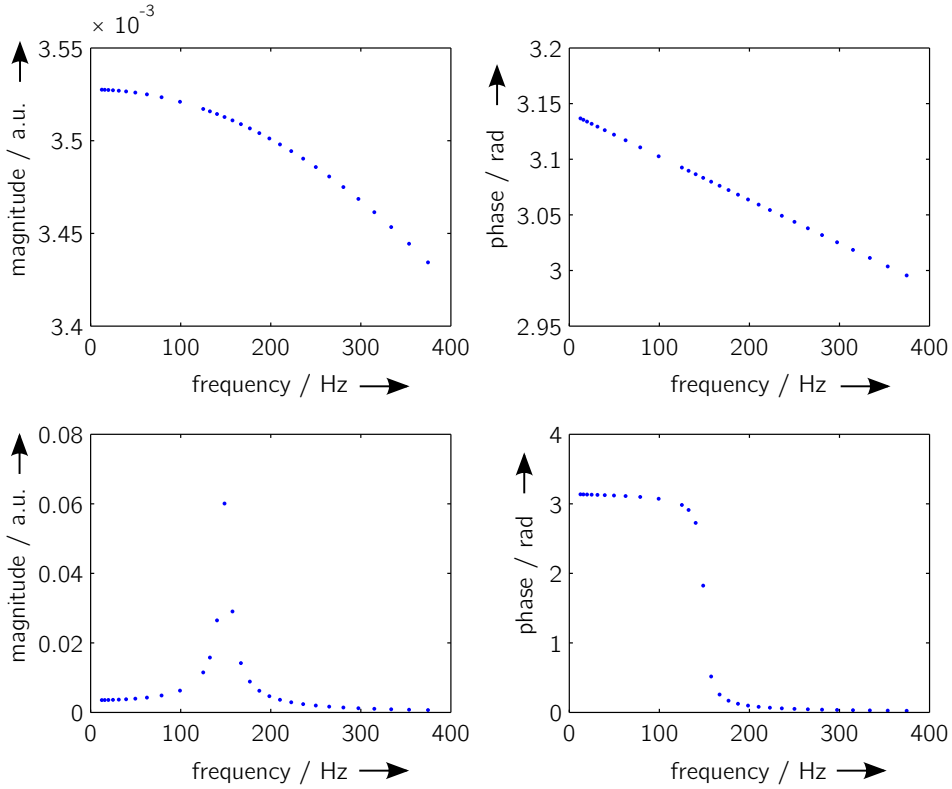

Figure 9: Simulation results for the 10 N · m shaft type transducer. Frequency response function H_{top} in magnitude and phase (top), frequency response function H_{bott} in magnitude and phase (bottom).

[3] **Bruns, T.**, *Sinusoidal Torque Calibration: A Design for Traceability in Dynamic Torque Calibration*, *Proc. of XVII IMEKO World Congress – Metrology in the 3rd Millennium*, Dubrovnik, Croatia, Jun. 2003.

[4] **ISO TC 43**, ISO 266:1997, Acoustics: Preferred frequencies for measurements, International Organization for Standardization (ISO), Geneva, Switzerland, 1997.

[5] **Klaus, L., Bruns, T.** and **Kobusch, M.**, *Determination of Model Parameters for a Dynamic Torque Calibration Device*, *Proc. of XX IMEKO World Congress*, Busan, Republic of Korea, Sep. 2012.

[6] **Klaus, L.** and **Kobusch, M.**, *Experimental Method for the Non-Contact Measurement of Rotational Damping*, *Proc. of Joint IMEKO International TC3, TC5 and TC22 Conference 2014*, Cape Town, South Africa, Feb. 2014.

[7] **Klaus, L., Arendacká, B., Kobusch, M.** and **Bruns, T.**, *Model Parameter Identification from Measurement Data for Dynamic Torque Calibration*, *Proc. of Joint IMEKO International TC3, TC5 and TC22 Conference 2014*, Cape Town, South Africa, Feb. 2014.

[8] **Beug, M. F., Moser, H.** and **Ramm, G.**, *Dynamic Bridge Standard for Strain Gauge Bridge Amplifier Calibration*, *Proc. of Conference on Precision Electromagnetic Measurements (CPEM)*, pp. 568–569, Washington, D.C., United States, Jul. 2012.

[9] **Klaus, L., Arendacká, B., Kobusch, M.** and **Bruns, T.**, *Dynamic Torque Calibration by Means of Model Parameter Identification*, ACTA IMEKO, 2014, submitted.